

Molecular Basis for Enantioselectivity of Lipase from *Chromobacterium viscosum* toward the Diesters of 2,3-Dihydro-3-(4'-hydroxyphenyl)-1,1,3-trimethyl-1*H*-inden-5-ol

David G. Gascoyne,[†] Herman L. Finkbeiner,[†] Kwok P. Chan,[†] Janet L. Gordon,[†]
Kevin R. Stewart,[†] and Romas J. Kazlauskas^{*,‡}

Molecular OptoElectronics Corporation, 877 25th Street, Watervliet, New York 12189, and
McGill University, Department of Chemistry, 801 Sherbrooke Street West,
Montréal, QC H3A 2K6 Canada

romas.kazlauskas@mcgill.ca

Received October 12, 2000

2,3-Dihydro-3-(4'-hydroxyphenyl)-1,1,3-trimethyl-1*H*-inden-5-ol, **1**, is a chiral bisphenol useful for preparation of polymers. Previous screening of commercial hydrolases identified lipase from *Chromobacterium viscosum* (CVL) as a highly regio- and enantioselective catalyst for hydrolysis of diesters of **1**. The regioselectivity was $\geq 30:1$ favoring the ester at the 5-position, while the enantioselectivity varied with acyl chain length, showing the highest enantioselectivity ($E = 48 \pm 20$ *S*) for the dibutanoate ester. In this paper, we use a combination of nonsymmetrical diesters and computer modeling to identify that the *remote* ester group controls the enantioselectivity. First, we prepared nonsymmetrical diesters of (\pm)-**1** using another regioselective, but nonenantioselective, reaction. Lipase from *Candida rugosa* (CRL) showed the opposite regioselectivity ($> 30:1$), allowing removal of the ester at the 4'-position (the remote ester in the CVL-catalyzed reaction). Regioselective hydrolysis of (\pm)-**1**-dibutanoate (150 g) gave (\pm)-**1**-5-dibutanoate (89 g, 71% yield). Acylation gave nonsymmetrical diesters that varied at the 4'-position. With no ester at the 4'-position, CVL showed no enantioselectivity, while hindered esters (3,3-dimethylbutanoate) reacted 20 times more slowly, but retained enantioselectivity ($E = 22$). These results indicate that the remote ester group can control the enantioselectivity. Computer modeling confirmed these results and provided molecular details. A model of a phosphonate transition state analogue fit easily in the active site of the open conformation of CVL. A large hydrophobic pocket tilts to one side above the catalytic machinery. The tilt permits the remote ester at the 4'-position of only the (*S*)-enantiomer to bind in this pocket. The butanoate ester fits and fills this pocket and shows high enantioselectivity. Both smaller and larger ester groups show low enantioselectivity because small ester groups cannot fill this pocket, while longer ester groups extend beyond the pocket. An improved large-scale resolution of **1**-dibutanoate with CVL gave (*R*)-(+)-**1**-dibutanoate (269 g, 47% yield, 92% ee) and (*S*)-(–)-**1**-4'-monobutanoate (245 g, 52% yield, 89% ee). Methanolysis yielded (*R*)-(+)-**1** (169 g, 40% overall yield, $> 97\%$ ee) and (*S*)-(–)-**1** (122 g, 36% overall yield, $> 96\%$ ee).

Introduction

Organic materials with nonlinear optical properties are the recent focus of both industrial and academic research due to the potential applications in telecommunications, optical information processing, storage and display.¹ Many nonlinear optical effects require a noncentrosymmetric, that is, chiral, environment for the chromophore. One way to create a chiral environment is to align the chromophore in poled polymer films or Langmuir–Blodgett films. A second way is to add chiral substituents to the chromophore. A third way is to create a chiral supramolecular array, such as a chiral liquid crystal or a chiral polymer. Devices with the strongest nonlinear optical effect often use several methods. For example, a Langmuir–Blodgett film of helicene showed a small nonlinear optical effect, but this effect increased ~ 30 -

fold when researchers used pure enantiomers of helicene in the film.² The pure enantiomers created a chiral supramolecular array similar to a liquid crystal. In another example, researchers used all three approaches. They added a chiral substituent to a chromophore, oriented it into a liquid crystal, poled it, and finally cross-linked this orientation.³

To use chiral polymers as supramolecular arrays in nonlinear optics requires polymers with good transparency and mechanical properties because they also form the mechanical shape of the device. Chiral polymers derived from polyacrylates or polystyrene with added chiral side chains⁴ have good transparency and mechanical properties, but the stereocenter lies far from the main chain. Chiral polymers with a stereocenter in the main chain would probably better control the polymer chain

* To whom correspondence should be addressed at McGill University. Phone: +1 514 398 7229, fax: +1 514 398 3797.

[†] Molecular OptoElectronics Corporation.

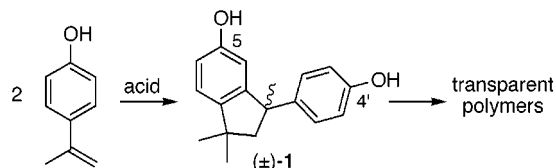
[‡] McGill University.

(1) Example: Nalwa, H. S.; Miyata, S., Eds. *Nonlinear Optics of Organic Molecules and Polymers*; CRC: Boca Raton, FL, 1997.

(2) Verbiest, T.; van Elshocht, S.; Kauranen, M.; Hellemans, L.; Snauwaert, J.; Nuckolls, C.; Katz, T. J.; Persoons, A. *Science* **1998**, *282*, 913–915.

(3) Trollsås, M.; Orrenius, C.; Sahlén, F.; Gedde, U. W.; Norin, T.; Hult, A.; Hermann, D.; Rudquist, P.; Komitov, L.; Lagerwall, S. T.; Lindström, J. *J. Am. Chem. Soc.* **1996**, *118*, 8542–8548.

Scheme 1. Carbenium Ion Mediated Dimerization of 4-(2-Propenyl)phenol Yields Racemic 2,3-Dihydro-3-(4'-hydroxyphenyl)-1,1,3-trimethyl-1*H*-inden-5-ol, (\pm)-1, a Bisphenol Monomer Useful for the Synthesis of Polymers



orientation. The ideal monomer would be rigid, contain a stereocenter within the main polymer chain, and form transparent polymers with excellent mechanical properties. Unfortunately, no such examples exist. One group recently reported binaphthol polycarbonates, but their molecular weights were very low.⁵

A monomer that fits these criteria is Indane bisphenol dimer or 2,3-dihydro-3-(4'-hydroxyphenyl)-1,1,3-trimethyl-1*H*-inden-5-ol, **1**. Acid-catalyzed dimerization of 4-propenylphenol,⁶ Scheme 1, yields racemic **1** in high yield. It also forms as an impurity in the commercial preparation of bisphenol A (2,2-bis(4-hydroxyphenyl)propane).⁷ Racemic **1** forms transparent polymers with good mechanical properties.⁸

We previously reported a regio- and enantioselective hydrolysis of diesters of **1**⁹ using lipase from *Chromobacterium viscosum*.¹⁰ Although chemists often resolve enantiomers using hydrolase-catalyzed reactions,¹² this reaction was unusual for two reasons. First, the hydrolysis was highly regio- and enantioselective despite the large distance between the stereocenter and ester car-

Table 1. Influence of the Acyl Group on the Enantioselectivity of CVL toward 1-Diesters

ester	rate (U/mg)	con- version (%) ^a	ee of mono- ester (%) ^b	<i>E</i> ^c
Straight Chain				
diacetate	15	63 ^d	42.3	5
dipropionate	11.5	37	78.5	14 ± 3
dibutanoate	8	36	93.2	48 ± 20 ^e
dipentanoate	11	39	92.4	35 ± 18 ^e
dihexanoate	0.4	51	78.4	21
diheptanoate	10	3.4	86.4	12
dioctanoate	2.8	8.8	63.8	5
dinonanoate	6.4	47	51.1	5
didecanoate	6.8	20	60.1	5
Branched Chain				
2-methylbutanoate	2	18	3.8	1.1
3-methylbutanoate	<1	<1	na	na
3,3-dimethyl-butanoate	<1	<1	na	na
Monoester				
5-butanoate	25	60 ^f	9 ^f	1.2
Nonsymmetrical Esters				
5-butanoate, 4'-3,3-dimethylbutanoate	0.4	3.8	91	22
5-butanoate, 4'benzoate	<1	<1	na	na

^a Measured by HPLC at 272 nm. Peak areas for the monoester were divided by 1.07 to account for the difference in extinction coefficient for diester and monoester. Data for the symmetrical, straight chain diesters is from ref 9. na = not applicable because the substrate did not react. ^b Hydrolysis forms the 4'-monoester in all cases. ^c Enantiomeric ratio as defined by Chen, C. S., Fujimoto, Y., Girdaukas, G., Sih, C. J. *J. Am. Chem. Soc.* **1982**, *104*, 7294–7299. ^d 2.6% diol noted in the hydrolysis of the diacetate. ^e Average and standard deviation for several different experiments or range for two experiments. ^f Conversion refers to the amount of diol formed; enantiomeric purity is for the diol.

bonyl at the 5-position (five bonds). Efficient resolutions of molecules containing stereocenter as remote as this one are rare.¹² Second, the enantioselectivity varied by approximately a factor of 10 (*E* = 5–50) with changes in the length of the acyl group.

In this paper we identify that the *remote*, nonreacting acyl group caused this variation in enantioselectivity. Further, we use molecular modeling to identify the molecular basis of the enantioselectivity. This is the first time that a molecular mechanism has been identified for the enantioselectivity toward such a remote stereocenter.

Results

Diesters. In the previous paper,⁸ we examined the effect of acyl group chain length on the enantioselectivity of CVL-catalyzed hydrolysis of **1**-diesters, Table 1. The dibutanoate ester (*E* = 48 ± 20) and dipentanoate ester (*E* = 35 ± 18) showed the highest enantioselectivity. Both shorter and longer esters showed lower enantioselectivity (e.g., *E* = 5 for both the diacetate and didecanoate). We also prepared several diesters of branched chain acids, Table 1, but they were disappointing. Branched chain diesters of **1** either did not react in CVL-catalyzed reactions (3-methylbutanoate, 3,3-dimethylbutanoate), or reacted slowly without enantioselectivity (2-methylbutanoate). Thus, the acyl groups influenced both the rate and enantioselectivity, but we did not know which acyl group caused these changes since we changed both simultaneously.

(4) For example, Chen, X. H.; Herr, R. P.; Schmitt, K.; Buchecker, R. *Liq. Cryst.* **1996**, *20*, 125–138; Firestone, M. A.; Park, J.; Minami, N.; Ratner, M. A.; Marks, T. J.; Lin, W.; Wong, G. K. *Macromolecules* **1995**, *28*, 2247–2259.

(5) Takata, T.; Furusho, Y.; Murakawa, K.; Endo, T.; Matsuoka, H.; Hirasa, T.; Matsuo, J.; Sisido, M. *J. Am. Chem. Soc.* **1998**, *120*, 4530–4531.

(6) Chan, K. P.; Cristo, P. L.; McGrath, P. M. US Patent 5,994,596, 1999.

(7) Paryzkova, J.; Snobl, D.; Matousek, P. *Chem. Prum.* **1979**, *29*, 30–34.

(8) For example, polycarbonates: Gordon, J. L.; Chan, K. P.; Gascoyne, D. G. *Polym. Prepr.* **1998**, *39*, 486–487; Gordon, J. L.; Gascoyne, D. G. US Patent 5,703,197, 1997; polyethers: Saegusa, Y.; Iwasaki, T.; Nakamura, S. *J. Polym. Sci., Part A: Polym. Chem.* **1994**, *32*, 249–256; polysiloxanes: Saegusa, Y.; Kato, T.; Oshiumi, H.; Nakamura, S. *J. Polym. Sci., Part A: Polym. Chem.* **1992**, *30*, 1401–1406; Padmanaban, M.; Kakimoto, M.; Imai, Y. *J. Polym. Sci., Part A: Polym. Chem.* **1990**, *28*, 2997–3005; polyesters: Wilson, J. C. *J. Polym. Sci., Polym. Chem. Ed.* **1975**, *13*, 749–754; Imai, Y.; Tassavori, S. *J. Polym. Sci., Polym. Chem. Ed.* **1984**, *22*, 1319–1325; Kakimoto, M.; Harada, S.; Oishi, Y.; Imai, Y. *J. Polym. Sci., Part A: Polym. Chem.* **1987**, *25*, 2747–2753; Negi, Y. S.; Imai, Y.; Kakimoto, M. *J. Polym. Mater.* **1988**, *5*, 67–71; Yoneyama, M.; Kakimoto, M.; Imai, Y. *Macromolecules* **1989**, *22*, 2593–2596; polyphosphates: Imai, Y.; Kamata, H.; Kakimoto, M. *J. Polym. Sci., Polym. Chem. Ed.* **1984**, *22*, 1259–1265.

(9) Zhang, M.; Kazlauskas, R. *J. Org. Chem.* **1999**, *64*, 7498–7503; Kazlauskas, R. J.; Zhang, X. U.S. Patent 5,959,159; 1999.

(10) Lipases from *Chromobacterium viscosum* and from *Pseudomonas glumae* have identical amino acid sequences and very similar biochemical properties. Taipal, M. A.; Liebeton, K.; Costa, J. V.; Cabral, J. M. S.; Jaeger, K.-E. *Biochim. Biophys. Acta* **1995**, *1256*, 396–402; Lang, D.; Hofmann, B.; Haalck, L.; Hecht, H. J.; Spener, F.; Schmid, R. D. *Schomburg, D. J. Mol. Biol.* **1996**, *259*, 704–717.

(11) (a) Faber, K. *Biotransformations in Organic Chemistry*, 4th ed.; Springer: Berlin, 2000. (b) Bornscheuer, U. T.; Kazlauskas, R. J. *Hydrolases in Organic Syntheses: Regio- and Stereoselective Biotransformations* Wiley-VCH: Weinheim, 1999. (c) Wong, C.-H.; Whitesides, G. M. *Enzymes in Synthetic Organic Chemistry*, Pergamon: Oxford, 1994.

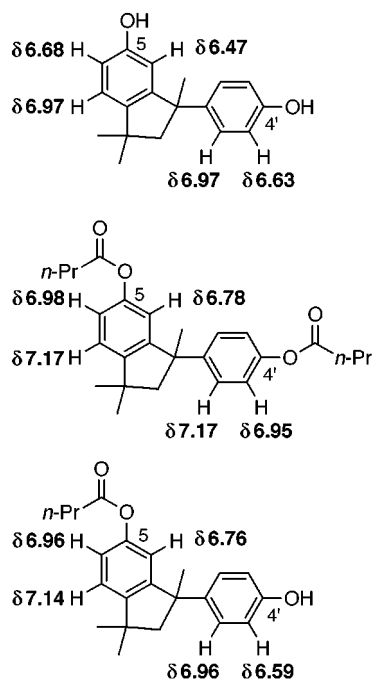
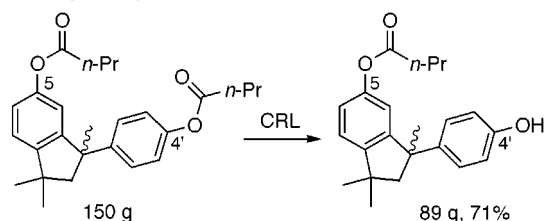


Figure 1. ^1H NMR chemical shifts of the aromatic protons in **1**,**1**-dibutanoate, and the **1**-monobutanoate isolated from a CRL-catalyzed hydrolysis of **1**-dibutanoate. The aromatic protons in **1** resonate 0.2–0.3 ppm upfield of those in **1**-dibutanoate. In the monobutanoate, the resonances of the less-substituted ring lie 0.21–0.36 ppm upfield from those in the dibutanoate, while those in the more-substituted ring lie at with 0.03 ppm of the dibutanoate. Thus, the ester group lies on the more substituted ring and is **1**-5-monobutanoate

Scheme 2. Regioselective Hydrolysis of the 4'-Ester Group by CRL Yields 1-5-Monobutanoate. This Hydrolysis Shows Low Enantioselectivity



1-5-Monobutanoate via Regioselective Hydrolysis 1-Dibutanoate. To identify which acyl group caused the changes in enantioselectivity, we needed racemic non-symmetrical diesters of **1**. Column chromatography on silica gel could not separate **1**-4'-monobutanoate and **1**-5-monobutanoate, so we used an enzyme-catalyzed regioselective reaction. The ideal reaction would be highly regioselective, but not enantioselective.

Our previous screening identified lipase from *Candida rugosa*, CRL, as a highly regioselective, but poorly enantioselective, catalyst.¹³ CRL favored hydrolysis of the 4'-ester group by >30:1, yielding **1**-5-monobutanoate, Scheme 2. The structure was established from the ^1H NMR chemical shifts, Figure 1. This regioselectivity is opposite that for CVL. Changing the acyl group in CRL-catalyzed reactions did not significantly change the regioselectivity (data not shown), but some acyl groups

Table 2. Enantioselectivity of CRL toward Several 1-Diesters

ester	rate (U/mg)	con-version (%) ^a	ee of mono-ester (%) ^b	<i>E</i> ^c
Straight Chain				
dibutanoate	5.3	52	33	3.7–4.7 ^d
dipentanoate	9.1	27	33	2.2
branched chain				
2-methylbutanoate	9.2	27	27	1.9
3-methylbutanoate	1.5	4.4	4.5	1.1
3,3-dimethylbutanoate	<1	<1	na	na
Nonsymmetrical Esters				
5-butanoate,	3.5	35	55	5.4
4'-3,3-dimethylbutanoate				
5-butanoate, 4'-benzoate	<1	<1	na	na

^a Measured by HPLC at 272 nm. Peak areas for the monoester were divided by 1.07 to account for the difference in extinction coefficient for diester and monoester. na = not applicable because the substrate did not react. ^b Hydrolysis forms the 5-monoester. ^c Enantiomeric ratio as defined by Chen, C. S., Fujimoto, Y., Girdaukas, G., Sih, C. J. *J. Am. Chem. Soc.* **1982**, *104*, 7294–7299. ^d Range for two experiments.

slightly changed the enantioselectivity, Table 2. As compared to the dipentanoate (*E* = 2.2), the enantioselectivity increased slightly for the dibutanoate (*E* = 3.7–4.7) and the nonsymmetrical ester 5-butanoate, 4'-3,3-dimethylbutanoate (*E* = 5.4), remained similar for the di(2-methylbutanoate) (*E* = 1.9) and decreased slightly for di(3-methylbutanoate) (*E* = 1.1). Two diesters did not react—the di(3,3-dimethylbutanoate) and the 5-butanoate, 4'-benzoate. This high regioselectivity combined with low enantioselectivity toward a wide range of esters make this a useful reaction for the preparation of **1**-5-monoesters.

We prepared **1**-5-monobutanoate by a CRL-catalyzed regioselective hydrolysis of the 4'-ester group in **1**-dibutanoate, Scheme 2. We allowed the CRL-catalyzed hydrolysis of (±)-**1**-dibutanoate (150 g) to proceed in an emulsion of *tert*-butyl methyl ether and water for 15 days until approximately 1 equiv of base had been consumed. This high conversion ensured that the product would be racemic. Workup of the reaction yielded the (±)-**1**-5-monobutanoate as a powder in 71% yield. We also prepared enantiomerically pure **1**-5-monobutanoate using the same reaction, but starting with enantiomerically pure **1**-dibutanoate. CRL-catalyzed hydrolysis of (*R*)-(+)-**1**-dibutanoate (22.4 g) yielded (*R*)-**1**-5-monobutanoate in 66% yield with >99% ee.

Nonsymmetrical Diesters. We prepared two non-symmetrical diesters where the ester at the 5-position (CVL-reactive) was butanoate and the ester at the 4'-position (CVL-nonreactive) was either 3,3-dimethylbutanoate or benzoate, Table 1. CVL-catalyzed hydrolysis of the nonsymmetrical ester with 3,3-dimethylbutanoate at the 4'-position was 20 times slower than the dibutanoate, but the enantioselectivity decreased only by a factor of 2 to *E* = 22. With a benzoate at the 4'-position, the butanoate at the 5-position no longer reacted. The most revealing case was the **1**-5-monobutanoate where there is no acyl group at the 4' position. The rate of CVL-catalyzed hydrolysis increased by a factor three, but the enantioselectivity disappeared (*E* = 1.2). Thus, structural changes remote from the reactive group affected both the rate and enantioselectivity of the CVL-catalyzed hydrolysis. We suggest therefore that variations of the remote

(13) Alternatively, one of the less enantioselective reactions catalyzed by CVL (e.g., diacetate) would yield the other regioisomer (the 4'-monoester). This route would involve protection–deprotection steps to prepare the 5-monoester, so we did not investigate it.

ester group caused most of the variations in enantioselectivity in the diester series.

Molecular Modeling. To rationalize why CVL favors the (*S*)-enantiomer and to provide details on how the remote ester group caused variations in enantioselectivity, we used computer modeling. First, we built a homology model of the open conformation of CVL. Although two groups have solved the X-ray crystal structure of CVL, both structures show the inactive closed conformation.¹⁴ On the other hand, crystallographers have solved the X-ray crystal structure of *Pseudomonas cepacia* lipase (PCL), a closely related lipase,¹⁵ in the active open conformation.¹⁶ These structures of CVL and PCL are almost identical, except for the position of the lid, a helical segment that blocks the active site in the closed conformation. This high degree of similarity suggests that we could build a reliable homology model of the open conformation of CVL based on the structure for PCL. We used Swiss-Model, an automated homology-modeling server,¹⁷ to create this model. As expected, the quality of this model was good with only a few high-energy orientations of side chains as identified by the program WhatCheck.¹⁸ The minimization below relaxed these high-energy orientations.

We built the phosphonate shown in Figure 2 into the active site of the open conformation of CVL. This phosphonate mimics the transition state for hydrolysis of 1-dibutanoate at the favored butanoate—at the 5-position of the (*S*)-enantiomer. The structure of **1** is relatively rigid and fit well into the alcohol-binding site. Energy minimization of this structure suggests a reasonable model for the transition state. The most interesting feature of this model is the location of the 4-butanoyloxyphenyl moiety in a large hydrophobic pocket. This pocket lies above the catalytic triad and tilts to the right. For the (*S*)-enantiomer, the 4-butanoyloxyphenyl moiety also tilts to the right and thus fits well in this pocket. In contrast, for the (*R*)-enantiomer (not shown), the 4-butanoyloxyphenyl moiety points to the left and lies outside the hydrophobic pocket. The calculated energy of the (*R*)-enantiomer complex lies 3.0 kcal/mol higher in energy than for the (*S*)-enantiomer complex, consistent with a less-favorable orientation for the (*R*)-enantiomer. An enantiomeric ratio of 48 corresponds to a free energy difference of 2.3 kcal/mol. Since the modeling ignores any

(14) Noble, M. E. M.; Cleasby, A.; Johnson, L. N.; Egmond, M. R.; Frenken, L. G. *J. FEBS Lett.* **1993**, *331*, 123–128; Lang, D. Hofmann, B. Haalck, L. Hecht, H. J. Spener, F. Schmid, R. D. Schomburg, D. J. *Mol. Biol.* **1996**, *259*, 704–717.

(15) The amino acid sequence of CVL (319 amino acids) differs from the sequence of PCL (320 amino acids) by fifty-one amino acids and one deletion. Of the fifty-one amino acids, thirty are highly conservative substitutions, twelve are conservative substitutions and only nine amino acids are different. Homology modeling of such similar proteins (84% identical amino acids, 97% similar amino acids) is very reliable. A reliability check showed that homology models deviated from the experimental structures by ≤ 2 Å deviation for the C α atoms in 79% of the cases and by ≤ 5 Å in 95% of the cases (Guex, N.; Diemand, A.; Peitsch, M. C. *Trends Biochem. Sci.* **1999**, *24*, 364–367.)

(16) Kim, K. K.; Song, H. K.; Shin, D. H.; Hwang, K. Y.; Suh, S. W. *Structure* **1997**, *5*, 173–185; Schrag, J. D.; Li, Y. G.; Cygler, M.; Lang, D. M.; Burgdorf, T.; Hecht, H. J.; Schmid, R.; Schomburg, D.; Rydel, T. J.; Oliver, J. D.; Strickland, L. C.; Dunaway, C. M.; Larson, S. B.; Day, J.; McPherson, A. *Structure* **1997**, *5*, 187–202; Lang, D. A.; Manesse, M. L. M.; De Haas, G. H.; Verheij, H. M.; Dijkstra, B. W. *Eur. J. Biochem.* **1998**, *254*, 333–340.

(17) Peitsch, M. C. *Bio/Technology* **1995**, *13*, 658–660; Peitsch, M. C. *Biochem. Soc. Trans.* **1996**, *24*, 274–279; Peitsch, M. C.; Guex, N. *Electrophoresis* **1997**, *18*, 2714–2723. <http://www.expasy.ch/swissmod/SWISS-MODEL.html>.

(18) Hooft, R. W. W.; Vriend, G.; Sander, C.; Abola, E. E. *Nature* **1996**, *381*, 272. <http://www.sander.embl-heidelberg.de/whatcheck/>.

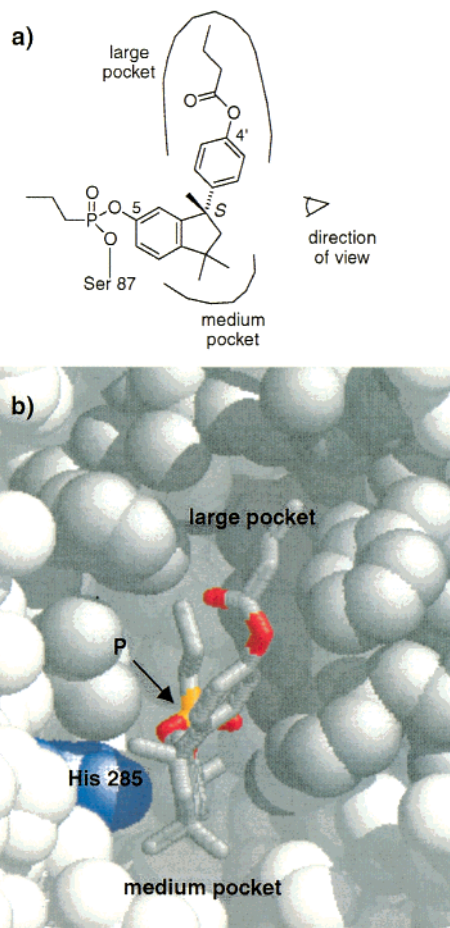
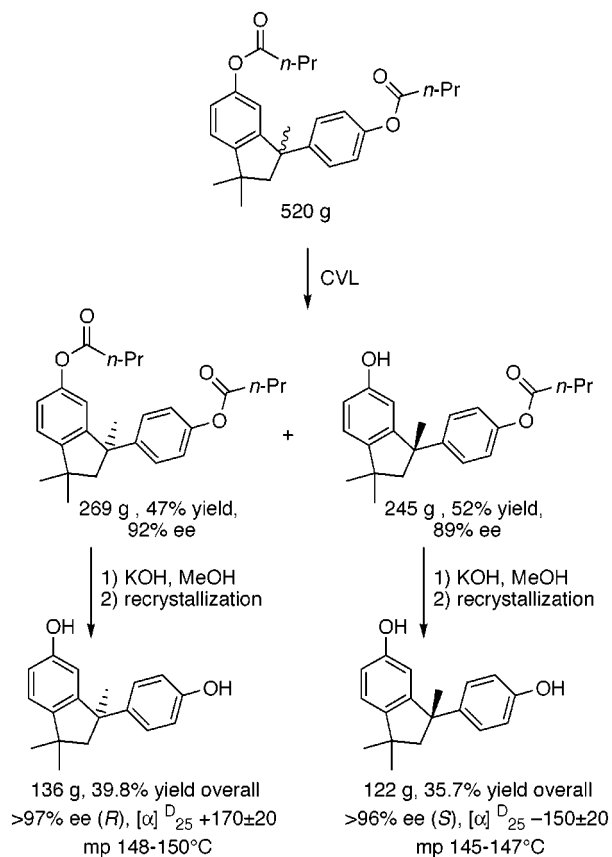


Figure 2. Molecular modeling of a transition state analogue in the active site of CVL rationalizes the observed preference for the (*S*)-enantiomer. (a) Line drawing of the phosphonate transition state analogue for the CVL-catalyzed hydrolysis of favored butanoyl group: 5-position of the (*S*)-enantiomer. This regioisomer and enantiomer is favored by $>30:1$ over other possibilities. Energy minimization of the structure yielded the orientation shown. The 4'-butanoyloxyphenyl group lay in the large hydrophobic pocket, while the CMe₂ group lay in the medium pocket. The “eye” shows the direction of view for part b. (b) Molecular model of the energy-minimized structure. The protein is shown in space-filling representation, while the transition state analogue is shown in stick representation. Hydrogens are omitted for clarity. The violet spheres represent the imidazole ring of the catalytic His 285. The medium gray spheres represent the nine hydrophobic residues in the active site: Leu 17, Phe 119, Val 123, Ile 139, Phe 142, Val 143, Phe 146, Leu 164, Leu 167. These residues line the large hydrophobic pocket, which lies above His 285 and tilts to the right. In the transition state analogue, red represents oxygen atoms, and an arrow points to the orange phosphorus atom. The 4'-butanoyloxyphenyl group fits and fills the large hydrophobic pocket. In the minimized structure for the other enantiomer the 4'-butanoyloxyphenyl group lies to the left, outside the large hydrophobic pocket. This difference in the orientation of the 4'-butanoyloxyphenyl group likely accounts for the faster reaction of the (*S*)-enantiomer. The starting protein structure was a homology model based on the open conformation of PCL, a lipase closely related to CVL.

entropy contributions, the agreement between the calculated 3.0 and the observed 2.3 kcal/mol is surprisingly good. Thus, this different binding of the 4-butanoyloxyphenyl moiety rationalizes the preference of CVL for the (*S*)-enantiomer. Note that PCL, which has a similar tilted large hydrophobic pocket, also favored the (*S*)-

Scheme 3. Large Scale Resolution of (\pm)-1 Dibutanoate Using the Regio- and Enantioselective Hydrolysis Catalyzed by CVL



enantiomer, but with lower enantioselectivity ($E \sim 10$).^{8,19} On the other hand, CRL, which has a roughly symmetrical large hydrophobic pocket, showed no enantioselectivity.

(R)-(+)-1 and (S)-(-)-1 via Large-Scale Resolution of (\pm)-1-Dibutanoate. To resolve (\pm)-1 on a large scale, we started with 408 g of (\pm)-1 and converted it to (\pm)-1-dibutanoate (568 g, 91% isolated yield). A portion of this diester (520 g) was hydrolyzed using CVL (Sigma) in a water and *tert*-butyl methyl ether emulsion to 48% conversion in 31 h, Scheme 3. Workup and separation of the mono- and dibutanoates by chromatography on silica gel yielded oils: (*R*)-(+)-1-dibutanoate, 269 g, 92% ee, 47% yield and (*S*)-(-)-1'-monobutanoate, 245 g, 89% ee, 52% yield. The enantiomeric ratio for this reaction was 56, better than the average for the small scale experiments in Table 2 above. The esters were saponified in basic methanol, and the resulting **1** was recrystallized from dichloromethane-methanol to give white crystals: (*R*)-(+)-**1**, 136 g, >97% ee, 40% yield and (*S*)-(-)-**1**, 122 g, >96% ee, 36% yield from the racemic dibutanoate. This recrystallization also raised the enantiomeric purity. The maximum yield in a resolution is 50%. This reaction was repeated to produce ~500 g of enantiomerically pure **1** for polymer synthesis.

Some organic compounds (~10%) crystallize as conglomerates and can be resolved by direct crystallization.²⁰ However, **1** does not crystallize as conglomerate. The

racemate melts significantly higher than the pure enantiomer: 193 vs 149 °C. For a conglomerate the racemate must melt at a lower temperature than the pure enantiomers. The racemate also shows a higher heat of fusion: 8.5 vs 6.8 kcal/mol. The predicted²¹ eutectic composition is 82% ee with a melting point of 143 °C. Lipase-catalyzed kinetic resolution remains the only route to pure enantiomers of **1**.

Discussion

In previous work,⁸ we identified CVL from Sigma as the most suitable hydrolase for preparation of pure enantiomers of **1**. CVL showed both high regioselectivity favoring the acyl group at the 5-position and high enantioselectivity for the (*S*)-enantiomer. Out of a number of different esters investigated, CVL showed the highest enantioselectivity toward the dibutanoate of **1** ($E = 48 \pm 20$). In this paper we reported a resolution of **1** on a larger scale and in higher yield than in previous work. This resolution is efficient and simple enough to prepare kilogram amounts of enantiomerically pure **1**.

In this paper, we also identified the molecular mechanism of enantioselectivity first by identifying which structural features are essential to enantioselectivity. Previously we noted that the acyl chain length in diesters of **1** affects the enantioselectivity, but did not know which of the two esters was more important. Here we varied the remote ester group (the ester that does not react in CVL-catalyzed reactions) and found it was crucial to the high enantioselectivity of CVL. We used a lipase with the opposite regioselectivity to remove the remote ester group. With no ester group at the 4'-position (**1**-5-monobutanoate), CVL showed no enantioselectivity, while with the corresponding diester (**1**-dibutanoate), CVL showed high enantioselectivity. This result suggests that the remote, nonreacting ester group is essential to high enantioselectivity.²² Consistent with this suggestion, the CVL-catalyzed hydrolysis of the nonsymmetrical diester—**1**-5-butanoate, 4'-3,3-dimethylbutanoate—showed good enantioselectivity, only a factor of 2 lower than **1**-dibutanoate.

To identify which structural features in CVL recognize this remote ester group, we used molecular modeling of a phosphonate transition state analogue. As expected, the chiral alcohol moiety **1** bound in the proposed alcohol-binding crevice. This crevice contains a large and a medium pocket. However, unlike many lipases such as CRL which have a roughly symmetrical large pocket, the large pocket in CVL is not symmetrical and tilts by ~30° to the right in Figure 2. Because of this tilt, the acyloxyphenyl moiety only for the (*S*)-enantiomer binds in the large pocket. Consistent with this explanation, CRL shows low enantioselectivity because its large pocket is roughly symmetrical, and PCL shows some enantioselectivity because its large pocket is also tilted. Further, size of this large pocket also suggests a reason the enantioselectivity of CVL varies with structural changes

(20) Jacques, J.; Collet, A.; Wilen, S. H. *Enantiomers, Racemates, and Resolutions*; Wiley-Interscience: New York, 1981.

(21) Reference 20, pp 88–93.

(22) We propose that the remote ester rather than the reactive ester is the more important for enantioselectivity. On the other hand, the reactive ester certainly influences the rate of reaction (e.g., no reaction for the **1**-di(3,3-dimethylbutanoate), but slow reaction for the **1**-5-butanoate, 4'-(3,3-dimethylbutanoate)) and may have a minor role in enantioselectivity.

(19) PCL was not suitable for preparative reactions because it showed low regioselectivity (less than approximately three favoring hydrolysis of the 5'-ester in **1**-dibutanoate).

in the remote ester group. With no acyl group or a small acyl group at the 4'-position, binding of the phenoxy or acyloxyphenyl group to the large hydrophobic pocket is weak. The (*S*)-enantiomer gains little advantage by having the correct tilt for the large pocket and the resulting enantioselectivity is low. Similarly, with a large acyl group (>C₆), only part of the acyl chain fits in the large pocket; the rest binds to the surface of the lipase for either enantiomer. Again difference in binding for the two enantiomers in low and the enantioselectivity is low. Only intermediate acyl groups (butanoate, pentanoate) maximize the difference in binding of the two enantiomers because the acyl group fits and fills the large pocket. Enantioselectivity is high for these intermediate acyl groups. This explanation is the first detailed proposal for how lipases recognize enantiomers with remote stereocenters.

The ready access to enantiomerically pure **1** will allow evaluation of enantiomerically pure polymers as matrixes for nonlinear optical devices. We have prepared polycarbonates and other polymers from **1**²³ and are measuring the properties of nonlinear optical devices and polarizing filters made from these chiral polymers.

Although the main focus of this work was the preparation of enantiomerically pure monomers to make chiral polymers for nonlinear optical applications, chiral polymers derived from **1** may also be useful as catalysts or catalyst supports for asymmetric synthesis.²⁴

Experimental Section

General. NMR spectra were recorded at 270 or 300 MHz in deuteriochloroform. Coupling constants are given in hertz. Mass spectra were obtained either by direct inlet electron ionization or by fast atom bombardment (6 kV Xe) in a glycerol matrix. THF was dried by distillation from sodium benzophenone ketyl under nitrogen. CVL was purchased from Sigma. Melting points and enthalpies of fusion for (±)-**1** and (−)-**1** were measured by differential scanning calorimetry. The eutectic composition was calculated as the intersection of the lines from the Schröder–van Laars equation, which predicts the part of the phase diagram lying between the pure enantiomer and the eutectic, and the Prigogine-Defay equation which predicts the phase diagram between the two eutectics.²⁰

(±)-**2,3-Dihydro-3-(4'-hydroxyphenyl)-1,1,3-trimethyl-1H-inden-5-ol**, (±)-**1**, was prepared by acid-catalyzed dimerization of 4-(2-propenyl)phenol.⁵

Symmetrical (±)-1-Diesters. Acid chloride (8.9 mmol, 2.4 eq) in dry THF (25 mL) was added over 10 min to a solution of **1** (1.0 g, 3.7 mmol) and triethylamine (0.90 g, 8.9 mmol, 2.4 eq) in dry THF (25 mL). TLC showed complete consumption of **1** after stirring overnight at room temperature. HCl (50 mL, 1 M) was added and the mixture was extracted with ethyl acetate (3 × 20 mL). The combined extracts were washed with NaHCO₃ (10%, 3 × 20 mL) and water (2 × 20 mL) and dried over magnesium sulfate. Chromatography on silica gel eluted with dichloromethane yielded colorless oils in 90–95% yield.

(±)-**1-Di(2-methylbutanoate)**: ¹H NMR δ 1.00 (m, 9H), 1.25 (m, 6H), 1.33 (s, 3H), 1.60 (m, 2H), 1.67 (s, 3H), 1.80 (m, 2H), 2.21 (d, 1H, *J* = 13), 2.38 (d, 1H, *J* = 13), 2.42 (d, 1H, *J* = 13), 2.59 (m, 2H), 6.79 (d, 1H, *J* = 6), 6.97 (m, 3H), 7.18 (m, 3H). ¹³C NMR δ 11.3, 11.4, 16.4, 26.6, 30.3, 30.5, 40.8, 40.9, 42.4, 50.2, 59.3, 117.7, 120.4, 120.8, 123.0, 127.4, 147.6, 148.5, 149.1, 149.7, 174.9, 175.0. HRMS (EI) Calcd for C₂₈H₃₆O₄ (M⁺) 436.26136, found 436.26134.

(±)-**1-Di(3-methylbutanoate)**: ¹H NMR δ 1.02 (m, 15H), 1.31 (s, 3H), 1.66 (s, 3H), 2.20 (m, 3H), 2.38 (m, 5H), 6.81 (d, 1H, 6), 6.97 (m, 3H), 7.17 (m, 3H). ¹³C NMR δ 22.0, 22.1, 25.5, 30.2, 30.3, 30.4, 42.2, 42.9, 43.0, 50.1, 59.2, 117.6, 120.4, 120.7, 122.9, 127.2, 147.5, 148.3, 149.0, 149.5, 171.0, 171.1. HRMS (EI) Calcd for C₂₈H₃₆O₄ (M⁺) 436.26136, found 436.26134.

(±)-**1-Di(2,2-dimethylpropanoate)**: ¹H NMR δ 1.05 (s, 3H), 1.32 (s, 12H), 1.34 (s, 9H), 1.67 (s, 3H), 2.21 (d, 1H, *J* = 13), 2.39 (d, 1H, *J* = 13), 6.78 (d, 1H, *J* = 2), 6.95 (m, 3H), 7.18 (m, 3H). ¹³C NMR δ 26.9, 27.0, 30.3, 30.5, 30.6, 38.8, 42.4, 50.2, 59.4, 117.6, 120.4, 120.7, 123.0, 127.4, 147.6, 148.7, 149.0, 149.7, 150.0, 176.8, 176.9. HRMS (EI) Calcd for C₂₈H₃₆O₄ (M⁺) 436.26136, found 436.26134.

(±)-**1-5-Monobutanoate via CRL-Catalyzed Regioselective Hydrolysis.** A solution of lipase from *Candida rugosa* (CRL, 9.0 mg solid, Sigma L 8525 dissolved in phosphate buffer, 0.1 M, 56 mL) was added to a solution of **1**-dibutanoate (150 g, 367 mmol, distilled under vacuum) in *tert*-butyl methyl ether (500 mL). The mixture was stirred to form an emulsion, and the pH was maintained at 7.2 by a pH stat, which controlled the addition of 5.0 M NaOH. After 13 d, 270 mmol of base was consumed and additional CRL (7.2 mg solid) was added. After 15 d, a total of 350 mmol of base was consumed and the stirring was stopped. The emulsion was allowed to settle and the water layer was discarded. The organic phase was washed with distilled water (2 × 250 mL) and concentrated to a gum by rotary evaporation followed by vacuum (800 μm Hg) at 120 °C. The gum was washed with hexane (200 mL), leaving a powder, 89 g, 71%. mp 123–126 °C, ¹H NMR δ 1.00 (m, 6H), 1.28 (s, 3H), 1.59 (s, 3H), 1.76 (sextet, 2H), 2.12 (d, 1H, *J* = 16), 2.36 (d, 1H, *J* = 16), 2.51 (t, 2H, *J* = 8), 6.36 (s, 1H, OH), 6.59 (d, 2H, *J* = 9), 6.76 (d, 1H, *J* = 2), 6.96 (m, 3H), 7.14 (broadened d, 1H, *J* = 8). ¹³C NMR δ 13.5, 18.3, 30.3, 30.5, 30.6, 36.2, 42.3, 49.9, 59.3, 114.7, 117.6, 120.3, 123.1, 127.5, 142.1, 149.5, 150.6, 153.6, 173.2. HRMS (EI) Calcd for C₂₂H₂₆O₃ (M⁺) 338.18819, found 338.18818.

(*R*)-(+)-**1-5-Monobutanoate via CRL-Catalyzed Regioselective Hydrolysis.** A similar procedure starting with (*R*)-(+)-**1**-dibutanoate (22.4 g, 54.8 mmol) yielded white powder, 12.3 g, 66%, >99% ee by HPLC on a Chiralcel AD column, mp 98–101 °C. The ¹H and ¹³C NMR were identical to those for the racemate.

Nonsymmetrical Diesters of (±)-1. Nonsymmetrical diesters were prepared by acylation of (±)-**1**-5-monobutanoate.

(×**b1**)±)-**1-5-Butanoate,4'-benzoate**: Benzoyl chloride (3.51 g, 33 mmol) was added to a solution of (±)-**1**-5-monobutanoate (7.1 g, 21 mmol) and triethylamine (2.55 g, 25 mmol) in *tert*-butyl methyl ether (20 mL), and the mixture was stirred for 2 h. The reaction mixture was washed with water (3 × 20 mL), dried over MgSO₄, and concentrated by rotary evaporation to an orange gum: 8.3 g, 90%; ¹H NMR δ 1.10 (m, 6H), 1.39 (s, 3H), 1.74 (s, 3H), 1.82 (m, 2H), 2.27 (d, 1H, *J* = 13), 2.48 (d, 1H, *J* = 13), 2.57 (t, 2H, *J* = 8), 6.86 (d, 1H, *J* = 2), 7.03 (dd, 1H, *J* = 2), 7.06 (dd, 1H, *J* = 2), 7.14 (d, 2H, *J* = 9), 7.22 (d, 2H, *J* = 8), 7.28 (d, 2H, *J* = 9), 7.53 (dd, 2H, *J* = 8), 7.63 (dd, 1H, *J* = 7), 8.23 (d, 2H, *J* = 8). ¹³C NMR δ 13.6, 18.4, 30.4, 30.6, 36.2, 42.5, 50.4, 59.4, 117.8, 120.6, 121.0, 123.2, 127.6, 128.5, 129.5, 130.0, 133.4, 148.0, 148.7, 149.3, 149.8, 149.9, 165.1, 172.2. HRMS (EI) Calcd for C₂₉H₃₀O₄ (M⁺) 442.21441, found 442.21439.

(±)-**1-5-Butanoate,4'-(2,2-dimethylpropanoate)**: The same procedure as above, but using 2,2-dimethylpropanoyl chloride. ¹H NMR δ 0.99 (m, 6H), 1.30 (m, 12H), 1.68 (m, 5H), 2.20 (d, 1H, *J* = 8), 2.43 (m, 3H), 6.84 (d, 1H, *J* = 2), 6.96 (m, 3H), 7.17 (m, 3H). ¹³C NMR δ 13.2, 17.9, 26.6, 30.0, 30.2, 35.6, 38.4, 42.0, 49.9, 59.0, 117.5, 120.3, 120.5, 122.8, 127.0, 147.2, 148.5, 148.7, 149.3, 149.5, 171.4, 176.1. HRMS (EI) Calcd for C₂₇H₃₄O₄ (M⁺) 422.24571, found 422.24569.

Large Scale Preparation of (±)-1-Dibutanoate. A 5-L, three-necked, round-bottom flask fitted with an overhead stirrer, a 250-mL addition funnel, and a water-cooled condenser was charged with a solution of racemic **1** (408 g, 1.52 mol) and triethylamine (338 g, 3.34 mol) in *tert*-butyl methyl ether (2.8 L). The flask was cooled in an ice bath while butanoyl chloride (356 g, 3.34 mol) was added over 1 h. After

(23) Gordon, J. L.; Stewart, K. R.; Chan, K. P. US Patent 5,777,063, 1998.

(24) Review: Pu, L. *Tetrahedron: Asymmetry* **1998**, *9*, 1457–1477; recent example: Yu, H.-B.; Hu, Q.-S.; Pu, L. *J. Am. Chem. Soc.* **2000**, *122*, 6500–6501.

stirring overnight at room temperature, HPLC analysis showed >99% **1**-dibutanoate. Water (1 L) was added to dissolve the suspended triethylamine hydrochloride. The mixture was transferred to a 6-L separatory funnel. The water layer was discarded, and the organic phase was washed with distilled water (2 × 500 mL), dried over MgSO₄, filtered, and concentrated to a yellow gum by rotary evaporation. Vacuum distillation (800 μm Hg) yielded a fraction boiling between 220 and 245 °C: oil, 568 g, 91%. HPLC and NMR showed >99% pure (±)-**1**-dibutanoate. ¹H NMR δ 1.06 (m, 10 H), 1.32 (s, 3H), 1.65 (s, 3H), 1.78 (m, 4H), 2.21 (d, 1H), 2.40 (d, 1H), 2.52 (dt, 4H), 6.78 (d, 1H, *J* = 2), 6.95 (d, 2H, *J* = 8), 6.98 (dd, 1H, *J* ~ 2, *J* ~ 8), 7.17 (two overlapping d, 3H, *J* ~ 8); MS (FAB, M+H⁺) 409.

520-g Scale Resolution of (±)-1-Dibutanoate. A 2-L, three-neck, round-bottom flask fitted with an overhead stirrer and a pH electrode connected to a pH controller was charged with (±)-**1**-dibutanoate (520 g, 1.27 mol), *tert*-butyl methyl ether (400 mL), and phosphate buffer (0.1 M, pH 7.5, 150 mL). After stirring to form an emulsion, a solution of CVL (40.8 mg, Sigma catalog no. L 0763, 120 000 units) in phosphate buffer (0.1 M, pH 7.5, 50 mL) was added. The pH controller maintained a pH of 7.2 by controlling the addition of 5.0 M NaOH. Aliquots (100 μL) for HPLC analysis (Chiralpak AD) were diluted in hexanes–ethanol (12: 1, 10 mL), dried over MgSO₄, and filtered through a 2 μm filter. After 31 h, 0.58 mol of base had been added and the solution contained 48.4 mol % (+)-**1**-dibutanoate, 50.4 mol % (–)-**1**-4'-monobutanoate (89% ee), and 1.2 mol % of diol **1**. The amount of base added (0.58 mol) is slightly less than expected from the HPLC analysis (0.67 mol).

The reaction mixture was transferred to a 3-L separatory funnel. *tert*-Butyl methyl ether (500 mL) and distilled water (500 mL) were added, the mixture was shaken, and the phases were allowed to separate (~15 min). The aqueous phase was discarded. The organic phase was washed with distilled water (2 × 500 mL) and concentrated first by rotary evaporation and then by heating under vacuum at 120 °C to give an orange gum, 479 g. This gum was dissolved in methylene chloride (250 mL) and chromatographed in six portions on silica gel (1.5 kg, 60–200 mesh) eluted first with dichloromethane. When the column effluent no longer contained (+)-**1**-dibutanoate (monitored by TLC), the solvent was switched to methanol to elute (–)-**1**-4'-monobutanoate. The column was repacked with virgin silica gel after each run. Removal of solvent from column fractions gave (+)-**1**-dibutanoate (yellow gum, 269 g) and (–)-**1**-4'-monobutanoate: orange gum, 245 g. ¹H and ¹³C NMR match those reported previously.⁸

(R)-(+)-1 and (S)-(–)-1. Solid KOH (1.2 mol for each molar equivalent of ester) was added to a 2-L, one-neck, round-bottomed flask containing (+)-**1**-dibutanoate (269 g) dissolved in methanol (500 mL). A strong exotherm heated the solution to reflux. The solution was stirred for 1 h at room temperature and then neutralized with an equivalent amount of concentrated HCl. Distilled water (500 mL) and *tert*-butyl methyl ether (500 mL) were added, and the mixture was transferred to a separatory funnel and shaken gently, and the phases allowed to separate. The aqueous layer was removed and saved. The organic phase was washed twice with distilled water (500 mL). All of the aqueous washes were combined and washed twice with *tert*-butyl methyl ether (500 mL). The combined organic phases were concentrated by rotary evaporation yielding (+)-**1** as a light brown solid, 194 g, 89% ee. A similar procedure yielded (–)-**1**, 224 g, 87% ee.

Solid (+)-**1** was recrystallized by dissolved in refluxing CHCl₃ (500 mL) and MeOH (50 mL). Cooling in the freezer overnight yield the first crop of crystals which were recovered by filtration, Table 3. The filtrate was concentrated to half its volume by rotary evaporation and cooled to room temperature. A fine powdery precipitate formed after 1 h and was recovered by filtration (crop 2). The remaining solution was cooled in the freezer overnight. A third crop of crystals was recovered by filtration. The remaining solution was concentrated by rotary evaporation, and the resulting solid was sublimed under vacuum to obtain a fourth crop of crystals: total of 136.3 g of

Table 3. Summary of Crystallization of Pure Enantiomers of **1^a**

crop	amount (g)	ee (%)
(R)-(+)-1		
1	88.6	99
2	20.8	28
3	40.4	97
4	7.3 ^b	97
total	136.3 g with >97% ee	
(S)-(–)-1		
1	79.8	96
2	40.4	24
3	42.5	97
4	c	77
total	122.3 g with >96% ee	

^a From chloroform–methanol (10:1). ^b By sublimation. ^c Not isolated.

(+)-**1** with >97% ee, 39.8% yield, [α]_D²⁰ +170 ± 20 (*c* = 3.9, MeOH), mp 148–150 °C (racemic mp 203–206 °C). Solid (–)-**1** was recrystallized in the same manner: total 122.3 g of (–)-**1** with >96% ee, 35.7% yield, [α]_D²⁰ –150 ± 20 (*c* = 4.1, MeOH), mp 145–147 °C. The maximum yield in a resolution is 50%.

Enantiomeric Purity. Enantiomers of **1** were separated on a Chiralcel OD HPLC column as reported previously.⁹ Enantiomers of **1**, the four isomers of **1**-monobutanoates and **1**-dibutanoate were also separated on two Chiralpak AD HPLC columns connected in series (Chiral Technologies Inc. Exton, PA) eluted with hexanes–ethanol (92/8, 1 mL/min): (±)-**1**-dibutanoate: *K* = 0.158; **1**-5-monobutanoate: α = 1.09, *K*_S = 0.563, *K*_R = 0.611; **1**-4'-monobutanoate: α = 1.11, *K*_R = 0.755, *K*_S = 0.838; **1**: α = 1.11, *K*_S = 2.25, *K*_R = 2.50. Enantiomers of the diesters did not separate on either the OD or the AD column. To determine the enantiomeric purity of **1**-diesters, they were cleaved with methanol/sodium methoxide, and the enantiomeric purity of the resulting **1** was determined as above.

Homology Model of the Open Conformation of CVL. We submitted the amino acid sequence of CVL (Swiss Prot code Q05489) and the open structure of PCL (Brookhaven protein databank code 1o1l) to Swiss-Model,¹⁶ an automated protein modeling server, where the structure was modeled using ProMod 2.0. A calcium ion was added manually to the calcium ion site between Asp241 and Asp 287. The structure did not have any water molecules. A check of this model using the program WhatCheck¹⁷ revealed a number of side chain atoms in high-energy orientations, but the minimizations below corrected these errors.

Modeling of Transition State Analogues in CVL. All modeling was done with *Discover*, version 2.9.7 (Biosym/MSI, San Diego, CA) using the Amber force field with a distance dependent dielectric constant of 4.0 and the 1–4 van der Waals interactions scaled by 50%. The distance dependent dielectric constant damps long-range electrostatic interactions to compensate for the lack of explicit solvation. Results were displayed using *Insight II* version 95.0 (Biosym/MSI). Protein structures in Figure 2 were created using RasMac v2.6.²⁵ Using the Biopolymer module of *Insight II*, hydrogen atoms were added to correspond to pH 7.0. Histidines were uncharged, aspartates and glutamates were negatively charged and arginines and lysines were positively charged. The catalytic histidine (His286) was protonated. The phosphonate transition state analogue was built manually and covalently linked to Ser 87. Energy minimization proceeded in four stages. First, 200 of iterations steepest descent algorithm, all protein atoms constrained with a force constant of 10 kcal mol^{–1} Å^{–2}; second, 200 iterations of conjugate gradients algorithm with the same constraints; and third, 500 iterations of conjugate gradients algorithm with only the backbone constrained by a 10 kcal mol^{–1} Å^{–2} force constant. For the fourth stage, minimization was continued using conjugate gradients algorithm without

any constraints until the rms deviation reached less than 0.005 Å mol⁻¹. The five expected hydrogen bonds between the transition state analogue and the catalytic amino acid residues were similar for both the (*R*)- and (*S*)-enantiomers, but two of these hydrogen bonds were significantly longer than the expected 3.0 ± 0.2 Å. The N–O distances between the main chain amide of Gln88 and the oxyanion was 3.4–3.5 Å, and this distance between the imidazole and the O-aryl was 3.8 Å. We attribute these long bonds to either the lack of water

molecules in the structure or inaccuracies in the homology model.

Acknowledgment. We thank the US Air Force for funding and NSERC (Canada) for the funds to purchase the modeling computer and software. We thank Michael (Xiaoming) Zhang for initial experiments with CRL.

JO005681V